platinum disrupts this relationship. Therefore intrastrand binding of a platinum ion across the N_7 position of two adjacent guanosines would significantly distort the structure of DNA at the binding site.

While the trans compound is also known to bind to DNA,[33] presumably at the N_7 position of guanosine, it is unable to bind to an adjacent guanosine due to the trans location of the second binding site. Thus upon binding to DNA, the trans complex leaves the DNA structure unaltered. We propose that the essential difference between *cis*-$Pt(NH_3)_2Cl_2$ and *trans*-$Pt(NH_3)_2Cl_2$ is the ability of the former to induce a localized distortion in the DNA structure which the trans complex cannot accomplish.

Registry No. *cis*-$[Pt(NH_3)_2(Guo)_2]Cl_{3/2}(ClO_4)_{1/2}\cdot 7H_2O$, 71911-91-6; *cis*-$[Pt(NH_3)_2(Ino)_2]Cl_2$, 50883-28-8; *cis*-$[Pt(NH_3)_2(Xao)_2]Cl_2$, 50790-43-7; *cis*-DDP, 15663-27-1.

Supplementary Material Available: A listing of structure factor amplitudes (12 pages). Ordering information is given on any current masthead page.

(41) S. Arnott, S. D. Dover, and A. J. Wonacott, *Acta Crystallogr., Sect. B*, **25**, 2192 (1969).

Contribution from the Laboratoire de Chimie de Coordination du CNRS associé à l'Université Paul Sabatier, 31400 Toulouse, France

Trinuclear "Crown-like" Metal Complexes: An Unusual Product of Reaction of Activated Alkynes with Dinuclear Thiolato-Bridged Iridium Complexes

J. DEVILLERS,† J.-J. BONNET, D. DE MONTAUZON, J. GALY, and R. POILBLANC*

Received April 17, 1978

The present work, supported by chemical, spectroscopic, and crystallographic studies, depicts the occurrence of oxidative additions of alkynes on initially nonbonded Ir(I) atoms of dinuclear complexes. Starting from $[Ir(\mu\text{-S-}t\text{-Bu})(CO)L]_2$ complexes, we obtained trinuclear complexes (L = CO) or dinuclear complexes (L = $P(OCH_3)_3$) both with a metal–metal bond (Ir(II)–Ir(II)). Special attention is devoted to the trinuclear species which exhibits a remarkable "crown-like" structure as shown by a crystal structure determination of $[Ir_3(\mu\text{-S-}t\text{-Bu})_3(\mu\text{-}C_4F_6)(CO)_6]$.

Introduction

In many dinuclear complexes, the alkyne ligand is μ-bridged to the metal atoms: the C–C bond is either perpendicular to the metal–metal axis as in $Co_2(CO)_6(RC_2R)$[1] or parallel as in $[Fe(\mu\text{-}SCF_3)(CO)_3]_2\cdot C_4F_6$.[2,3]

In iridium(I) chemistry, an original dinuclear complex $[Ir(\mu\text{-Cl})(C_8H_{12})(C_4F_6)]_2$ has been recently reported:[4] in this complex, alkyne (and alkene) ligands are coordinated to the same metal atom.

As part of our continuing interest in the coordination chemistry of new iridium carbonyl compounds $[Ir(\mu\text{-S-}t\text{-Bu})(CO)L]_2$ (L = CO or $P(OCH_3)_3$) recently described,[5] we have investigated the reaction of hexafluorobut-2-yne and dimethylacetylene dicarboxylate with these complexes. We now report the synthesis and the characterization of an unusual type of trinuclear iridium complex.

Experimental Section

Physical Measurements. The infrared spectra were recorded with a Perkin-Elmer 225 grating apparatus. Hexadecane solution or cesium bromide dispersions were used. In the ν_{CO} region of interest, the spectra were calibrated by water vapor lines. Proton NMR spectra have been run on Varian A60A and fluorine NMR spectra run on a Perkin-Elmer R10. Microanalyses were carried out by the Service Central de Microanalyses du CNRS. Melting points were determined in air. Molecular weights were determined by tonometry in benzene by using a Mechrolab apparatus. Magnetic measurements were obtained by using the Faraday method with $HgCo(SCN)_4$ as standard ($\chi_g = 16.44 \times 10^{-6}$ cgsu).

Preparation of Complexes. $[Ir(\mu\text{-S-}t\text{-Bu})(CO)_2]_2$ (I) and $[Ir(\mu\text{-S-}t\text{-Bu})(CO)(P(OCH_3)_3)]_2$ (II) were prepared as previously described.[5]

Preparation of $[Ir_3(\mu\text{-S-}t\text{-Bu})_3(\mu\text{-}C_4F_6)(CO)_6]$ (III). In a typical reaction, 1.012 g of I (ca. 1.5 mmol) was transferred to a thick glass reaction vessel fitted with a Teflon stopcock. It was evacuated and cooled to −196 °C, and pentane (ca. 20 mL) and hexafluorobut-2-yne (ca. 0.2 g) were condensed in. The reaction mixture was then allowed to warm-up slowly to room temperature and was stirred overnight. The solution was then evaporated under reduced pressure. By crystallization at −40 °C in toluene, lemon yellow crystals were obtained and vacuum dried. A 0.950-g amount of product was obtained: yield ~80%; mp 148 °C; $\chi_M = -509.9 \times 10^6$ cgsu.

Anal. Calcd for $Ir_3C_{22}H_{27}O_6S_3F_6$: C, 22.50; H, 2.30; S, 8.18; F, 9.70. Found: C, 22.26; H, 2.30; S, 8.05; F, 9.80. Molecular weight: calcd, 1174; found, 1180.

Preparation of $[Ir_3(\mu\text{-S-}t\text{-Bu})_3(\mu\text{-}C_2(CO_2CH_3)_2)(CO)_6]$ (IV). To a solution of 1.012 g of I (1.5 mmol) in 20 mL of pentane was added 0.142 g (0.123 mL) of $C_2(CO_2CH_3)_2$. The solution was stirred overnight. By crystallization at −40 °C in pentane, orange crystals (0.922 g, yield ~80%) were obtained and dried in vacuo; mp 142 °C dec.

Anal. Calcd for $Ir_3C_{24}H_{33}O_{10}S_3$: C, 24.98; H, 2.86; S, 8.33. Found: C, 25.08; H, 2.95; S, 8.03. Molecular weight: calcd, 1153; found, 1172.

Preparation of $[Ir_2(\mu\text{-S-}t\text{-Bu})_2(\mu\text{-}C_4F_6)(CO)_2(P(OCH_3)_3)_2]$ (V). In a typical reaction 0.867 g (ca. 1 mmol) of II[5] was transferred to a thick glass reaction vessel fitted with a Teflon stopcock. It was evacuated and cooled to −196 °C and pentane (ca. 50 mL) and the alkyne (ca. 0.2 g) were condensed in. The reaction mixture was then allowed to warm slowly to room temperature and was stirred overnight. The solution was evaporated under reduced pressure. By crystallization at −40 °C in a CH_2Cl_2–hexane (1:1) mixture, lemon yellow crystals were obtained and vacuum dried. A 0.800-g amount of product was obtained: yield ~80%; mp 165 °C dec; $\chi_M = -430.1 \times 10^{-6}$ cgsu; λ_{max} 315 nm (ϵ 7480 M^{-1} cm^{-1} (in CH_2Cl_2 solution)).

Anal. Calcd for $Ir_2C_{20}H_{36}O_8P_2S_2F_6$: C, 23.34; H, 3.50; S, 6.23; F, 11.07. Found: C, 23.59; H, 3.57; S, 6.22; F, 11.10. Molecular

† Equipe de Recherche du CNRS No. 82 (Université Paul Sabatier).

(1) R. S. Dickson and J. P. Fraser, *Adv. Organomet. Chem.*, **12**, 323 (1974), and references therein.
(2) J. L. Davidson, W. Harrison, D. W. A. Sharp, and G. A. Sim, *J. Organomet. Chem.*, **46**, C47 (1972).
(3) R. Mathieu and R. Poilblanc, *J. Organomet. Chem.*, **142**, 351 (1977).
(4) D. R. Russel and A. Tucker, *J. Organomet. Chem.*, **125**, 303 (1977); D. A. Clarke, R. D. W. Kemmitt, D. R. Russel, and P. Tucker, *ibid.*, **93**, C37 (1975).
(5) J.-J. Bonnet, J. Galy, D. de Montauzon, and R. Poilblanc, *J. Chem. Soc., Chem. Commun.*, 47 (1977).

0020-1669/80/1319-0154$01.00/0

Table I. Physical and Crystallographic Data of $Ir_3(\mu\text{-}SC_4H_9)_3(\mu\text{-}C_4F_6)(CO)_6$ and Experimental Conditions of Crystallographic Measurements

1. Physical and Crystallographic Data

formula: $Ir_3(\mu\text{-}S\text{-}t\text{-}Bu)_3(\mu\text{-}C_4F_6)(CO)_6$	mol wt: 1174.23
cryst system: triclinic	space group: $P\bar{1}$
$a = 11.891$ (1) Å	$V = 1584.3$ Å^3
$b = 12.154$ (2) Å	$Z = 2$
$c = 11.448$ (3) Å	$F(000) = 540$
$\alpha = 106.75$ (6)°	$\rho_{exptl} = 2.42$ (1) g cm^{-3}
$\beta = 90.07$ (6)°	$\rho_{calcd} = 2.46$ g cm^{-3}
$\gamma = 89.99$ (4)°	$\mu(\lambda Mo) = 135.6$ cm^{-1}

2. Data Collection

temp: 21 °C
radiation: molybdenum; $\lambda(K\bar{\alpha})$ 0.710 69 Å
monochromatization: oriented graphite crystal
crystal–detector distance: 208 mm
detector window:[a] height = 4 mm; width = 4.00 + 0.00 tan θ
takeoff angle:[a] 3.7°
scan mode: θ/ω
max Bragg angle: 28°
values determining the scan speed: first shell ($2° \leq \theta \leq 20°$) SIGPRE[a] = 0.33, SIGMA[a] = 0.02, VPRE[a] = 10° min^{-1} for θ, TMAX[a] = 45 s; second shell ($20° < \theta \leq 26°$) SIGPRE[a] = 0.33, SIGMA[a] = 0.02, VPRE[a] = 15° min^{-1} for θ, TMAX[a] = 60 s; third shell ($26° < \theta \leq 28°$) SIGPRE[a] = 0.33, SIGMA[a] = 0.02, VPRE[a] = 15° min^{-1} for θ, TMAX[a] = 60 s
intens controls: 434, 640, 066, 241 measured every 8000 s of irradiation

3. Conditions for Refinement

reflctns for the refinement of the cell dimensions: 25
recorded reflctns: 7601
independent reflctns: 7601
utilized reflctns: $(>3\sigma(I)) = 5695$
reliability factors: $R = \Sigma|k|F_o| - |F_c||/\Sigma k|F_o|$; $R_w = [\Sigma w(k|F_o| - |F_c|)^2/\Sigma wk^2F_o^2]^{1/2}$
std error in an observn of unit weight: 1.72

[a] Values specified in ref 6.

weight: calcd, 1029; found, 1051.

Preparation of $[Ir_2(\mu\text{-}S\text{-}t\text{-}Bu)_2(\mu\text{-}C_2(CO_2CH_3)_2)(CO)_2(P(OCH_3)_3)_2]$ (VI). To a solution of 0.867 g (1 mmol) of II[5] in 50 mL of pentane was added 0.142 g (0.123 mL) of $C_2(CO_2CH_3)_2$. Upon stirring of the mixture for 30 min, a lemon yellow powder precipitates. By crystallization at −40 °C in a toluene–hexane (1:5) mixture, yellow crystals (0.800 g, yield ~80%) were obtained and dried in vacuo; mp 154 °C.

Anal. Calcd for $Ir_2C_{22}H_{42}O_{12}P_2S_2$: C, 26.19; H, 4.36; S, 6.34. Found: C, 26.40; H, 4.21; S, 5.96. Molecular weight: calcd, 1009; found, 1000.

Crystallographic Study. Examination of crystals of $Ir_3(\mu\text{-}S\text{-}t\text{-}Bu)_3(\mu\text{-}C_4F_6)(CO)_6$ by precession methods with Mo Kα radiation failed to reveal the presence of any symmetry element but the center of symmetry imposed by Friedel's law; hence, the space group is either $P1$ or $P\bar{1}$. The setting angles of 25 *hkl* reflections, regularly distributed in the half sphere, automatically centered on a Nonius CAD 4 diffractometer, were used in a least-squares calculation which led to the cell constants (Table I). On the assumption of two formula units per cell, the calculated density $\rho_{calcd} = 2.46$ g cm^{-3} is in satisfactory agreement with the experimental one $\rho_{exptl} = 2.42$ g cm^{-3} measured by flotation in a ZnI_2 aqueous solution.

Data Collection. Table I gives pertinent details concerning the experimental data collection conditions. Reflections have been recorded in three shells with the same crystal. Examination of the control reflection intensities, periodically measured, showed an isotropic, continuous, and linear decrease of intensity, up to 4.3% from the initial values during the collection of the first shell and up to 14.8% for the second and third shells. A linear correction has been applied to the data to take into account this decrease. Data were then processed in the normal way[6] by using a value of $p = 0.03$.

Absorption corrections have been carried out by using a numerical method.[7] The crystal selected for data collection was a parallelepiped

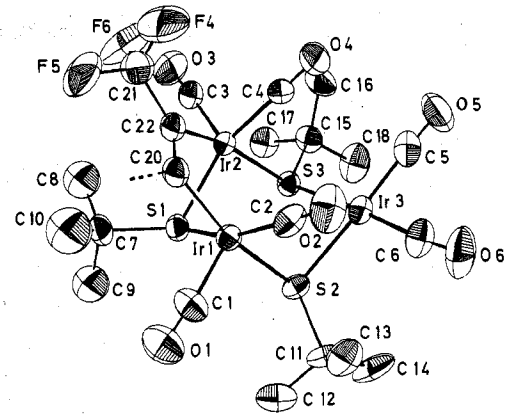

Figure 1. Perspective view and labeling scheme of the molecule $Ir_3(\mu\text{-}S\text{-}t\text{-}Bu)_3(\mu\text{-}C_4F_6)(CO)_6$. For the sake of clarity, the group C(19)F(1)F(2)F(3) linked to C(20) and the disorder of the *tert*-butyl group linked to S(1) (atoms C′(8), C′(9), C′(10)) have been omitted as well as hydrogen atoms. Thermal ellipsoids are scaled to include 50% probability.

with bounding faces of the forms $\{0\bar{1}1\}$, {100}, and {011}. The distances between the faces of these forms are 0.331, 0.166, and 0.067 mm. On the basis of a linear absorption coefficient of 135.6 cm^{-1}, the resultant transmission factors were found to range from 0.593 to 0.877.

Structure Determination. The structure has been solved by standard Patterson and Fourier methods. Conditions of refinement and the used agreement indices R and R_w are defined in Table I. Values of the atomic scattering factors and the anomalous terms used for Ir and S were from usual sources.[8] Initially it was assumed that the correct space group is the centrosymmetric one, $P\bar{1}$, rather than its noncentrosymmetric subgroup $P1$.

From the Patterson function the three Ir atoms were located, and on a subsequent Fourier map, the three S atoms and four carbonyl groups were found. The next Fourier map allowed us to attribute the observed density maxima to all the remaining heavy atoms but the carbon atoms (C(8), C(9), C(10)) of the S(1)-*t*-Bu group. A least-squares refinement using isotropic thermal parameters for 37 heavy atoms led to $R = 0.08$ and $R_w = 0.09$. At this point a difference Fourier map in an oblique plane perpendicular to the S(1)–C(7) bond showed clearly that the carbon atoms of the S(1)-*t*-Bu group are disordered occupying two alternate positions. Further full-matrix least-squares cycles of refinement were performed by using anisotropic thermal parameters for all heavy atoms except the disordered carbon ones, the parameters of which were refined with isotropic thermal parameters and with fixed occupancy factors of 0.5. R and R_w were both equal to 0.049.

In the next difference Fourier maps, calculated in oblique planes, hydrogen atoms of the S(2)-*t*-Bu and S(1)-*t*-Bu groups were localized. Their positions were idealized (C–H = 1.01 Å) through a least-squares calculation.[7] Their contributions to F_c were then fixed during the final cycles of refinement which included an isotropic secondary extinction correction. For each hydrogen atom, an isotropic thermal parameter was assigned with a value 1 Å^2 greater than that of the C atom to which it is attached. Last values of R and R_w were both equal to 0.044. A final difference Fourier electron density map revealed nine peaks of density ranging from 1.0 to 1.3 e Å^{-3} (15.6–20% of the density of a carbon atom). The two highest ones at distances of 1.3 Å from the Ir(1) and Ir(2) atoms were located in the area away

(6) A. Mosset, J.-J. Bonnet, and J. Galy, *Acta Crystallogr., Sect. B*, **33**, 2639 (1977).

(7) All calculations have been performed by using the CII IRIS 80 computer of the "Centre Interuniversitaire de Calcul de Toulouse". In addition to various local programs, modified versions of the following ones were employed: Ibers' AGNOST absorption program which includes both the Coppens–Leiserowitz–Rabinovich logic for Gaussian integration and the Tompa–de Meulenaur analytical method; Zalkin's FORDAP Fourier summation program; Johnson's ORTEP thermal ellipsoid plotting program; Busing and Levy's ORFFE error function program; Ibers' NUCLS full-matrix least-squares program, which in its nongroup form resembles the Busing and Levy's ORFLS program; HYDRA, which idealizes H atoms of CH_3 groups through a least-squares calculation (C–H = 1.01 Å).

(8) D. T. Cromer and J. T. Waber, "International Tables for X-ray Crystallography", Vol. IV, Kynoch Press, Birmingham, England, 1974, Table 2.2.A.

Table II. Positional and Thermal Parameters for the Atoms of $Ir_3(\mu\text{-}SC_4H_9)_3(\mu\text{-}C_4F_6)(CO)_6$[a]

atoms	x	y	z	U_{11}	U_{22}	U_{33}	U_{12}	U_{13}	U_{23}
Ir(1)	0.14802 (3)	0.15012 (3)	−0.17086 (4)	3.80 (2)	3.33 (2)	3.71 (2)	0.43 (1)	0.14 (1)	1.03 (2)
Ir(2)	0.31333 (3)	0.21041 (3)	−0.30067 (4)	3.37 (2)	4.11 (2)	3.29 (2)	0.74 (1)	0.01 (1)	1.18 (2)
Ir(3)	0.03696 (3)	0.29359 (4)	−0.37751 (4)	3.83 (2)	3.86 (3)	4.73 (3)	0.16 (2)	−0.65 (2)	1.27 (2)
S(1)	0.2872 (2)	0.2899 (2)	−0.0898 (2)	4.0 (1)	4.3 (1)	3.7 (1)	0.1 (1)	−0.62 (10)	1.0 (1)
S(2)	0.0272 (2)	0.3167 (2)	−0.1642 (2)	3.7 (1)	3.5 (1)	4.9 (2)	0.56 (9)	0.6 (1)	1.1 (1)
S(3)	0.2127 (2)	0.3844 (2)	−0.3117 (2)	3.8 (1)	3.8 (1)	4.0 (1)	0.15 (9)	−0.10 (10)	1.5 (1)
F(1)	0.282 (1)	−0.088 (1)	−0.080 (1)	27 (2)	10.8 (9)	12 (1)	−3.2 (9)	−4.7 (10)	8.3 (8)
F(2)	0.312 (1)	−0.1742 (8)	−0.252 (1)	24 (1)	5.5 (6)	26 (2)	6.8 (7)	14 (1)	6.9 (8)
F(3)	0.1508 (8)	−0.1234 (9)	−0.197 (1)	8.5 (6)	8.6 (7)	32 (2)	−1.7 (5)	−2.4 (8)	12.0 (9)
F(4)	0.4442 (9)	−0.090 (1)	−0.422 (1)	13.3 (8)	13.7 (9)	10.4 (8)	6.9 (7)	1.5 (6)	−3.2 (7)
F(5)	0.5020 (8)	−0.064 (1)	−0.244 (1)	12.0 (7)	20 (1)	14.1 (10)	10.8 (8)	4.3 (6)	10.8 (9)
F(6)	0.5411 (7)	0.0519 (9)	−0.336 (1)	7.5 (5)	10.5 (8)	21 (1)	4.7 (5)	6.2 (7)	6.1 (8)
O(1)	0.0760 (9)	0.0986 (9)	0.0615 (10)	10.7 (8)	9.1 (8)	7.1 (7)	−0.7 (6)	0.9 (6)	4.1 (6)
O(2)	0.0015 (7)	−0.0109 (7)	−0.3598 (9)	7.8 (6)	4.6 (5)	9.5 (8)	−1.0 (4)	−3.0 (5)	0.8 (5)
O(3)	0.5505 (7)	0.2900 (9)	−0.3379 (9)	4.9 (5)	10.0 (8)	9.1 (8)	0.2 (5)	0.6 (5)	2.9 (6)
O(4)	0.2536 (7)	0.0787 (8)	−0.5593 (8)	6.9 (5)	7.8 (6)	4.7 (5)	1.4 (4)	−1.1 (4)	−0.6 (5)
O(5)	0.0593 (8)	0.273 (1)	−0.6411 (9)	9.8 (7)	12.5 (10)	4.4 (6)	−1.9 (6)	−1.6 (5)	2.5 (6)
O(6)	−0.1880 (8)	0.188 (1)	−0.451 (1)	6.6 (6)	12.1 (9)	11.5 (9)	−3.5 (6)	−4.4 (6)	5.6 (7)
C(1)	0.097 (1)	0.117 (1)	−0.027 (1)	7.9 (8)	5.6 (8)	4.5 (7)	−0.1 (6)	0.2 (6)	1.9 (6)
C(2)	0.0548 (9)	0.051 (1)	−0.288 (1)	4.2 (5)	4.6 (7)	7.0 (8)	0.8 (5)	0.2 (5)	1.6 (6)
C(3)	0.4618 (9)	0.2594 (10)	−0.326 (1)	5.4 (6)	5.4 (7)	4.7 (7)	1.4 (5)	−0.2 (5)	1.8 (5)
C(4)	0.2757 (8)	0.1292 (10)	−0.4644 (10)	4.5 (5)	5.2 (7)	3.7 (6)	1.4 (5)	0.2 (4)	0.4 (5)
C(5)	0.0536 (10)	0.282 (1)	−0.541 (1)	5.7 (7)	5.6 (8)	6.2 (9)	−0.2 (5)	−1.7 (6)	1.7 (6)
C(6)	−0.1038 (9)	0.230 (1)	−0.418 (1)	5.2 (6)	5.5 (7)	7.8 (9)	−0.3 (5)	−1.6 (6)	2.9 (7)
C(7)	0.3936 (10)	0.267 (1)	0.021 (1)	6.0 (7)	6.6 (8)	3.9 (6)	0.9 (6)	−1.4 (5)	0.8 (6)

atoms	x	y	z	B, Å^2	atoms	x	y	z	B, Å^2
C(8)	0.510 (2)	0.284 (3)	−0.027 (3)	6.9 (7)	C′(8)	0.333 (2)	0.277 (3)	0.135 (3)	6.5 (7)
C(9)	0.362 (2)	0.361 (3)	0.142 (3)	6.9 (7)	C′(9)	0.466 (2)	0.160 (3)	−0.022 (3)	6.0 (6)
C(10)	0.393 (3)	0.149 (4)	0.040 (4)	9 (1)	C′(10)	0.476 (3)	0.376 (3)	0.028 (3)	7.7 (8)

atoms	x	y	z	U_{11}	U_{22}	U_{33}	U_{12}	U_{13}	U_{23}
C(11)	−0.1159 (8)	0.3075 (10)	−0.100 (1)	4.3 (5)	4.7 (7)	6.6 (8)	0.7 (5)	2.6 (5)	1.2 (6)
C(12)	−0.098 (1)	0.342 (1)	0.038 (1)	7.6 (8)	7.3 (10)	6.7 (10)	0.5 (7)	2.6 (7)	0.9 (7)
C(13)	−0.1689 (9)	0.188 (1)	−0.144 (1)	4.7 (6)	6.2 (8)	9 (1)	−1.7 (6)	−0.2 (6)	2.7 (7)
C(14)	−0.1860 (10)	0.397 (1)	−0.135 (2)	4.9 (6)	7.7 (10)	12 (1)	3.3 (6)	3.7 (7)	3.7 (9)
C(15)	0.2767 (9)	0.4624 (9)	−0.413 (1)	5.6 (6)	4.5 (6)	4.7 (7)	−0.2 (5)	0.3 (5)	2.5 (5)
C(16)	0.323 (1)	0.383 (1)	−0.531 (1)	7.8 (8)	9 (1)	4.2 (7)	−0.1 (7)	0.8 (6)	2.7 (7)
C(17)	0.3708 (10)	0.535 (1)	−0.334 (1)	5.9 (7)	5.7 (8)	6.9 (9)	−0.9 (6)	−0.2 (6)	2.1 (7)
C(18)	0.188 (1)	0.542 (1)	−0.436 (1)	8.2 (9)	5.8 (8)	10 (1)	−0.2 (7)	−1.5 (8)	5.4 (8)
C(19)	0.252 (1)	−0.090 (1)	−0.187 (1)	8.0 (9)	5.9 (9)	8 (1)	1.9 (7)	1.2 (7)	3.8 (8)
C(20)	0.2704 (9)	0.0221 (9)	−0.2141 (10)	5.5 (6)	4.5 (6)	4.1 (6)	1.2 (5)	−0.1 (5)	1.9 (5)
C(21)	0.457 (1)	−0.015 (1)	−0.319 (1)	8.4 (9)	8.0 (10)	6.2 (9)	3.5 (8)	1.9 (7)	4.2 (8)
C(22)	0.3517 (9)	0.0532 (9)	−0.2717 (10)	5.3 (6)	4.8 (6)	3.9 (6)	1.7 (5)	−0.1 (5)	1.5 (5)

[a] Estimated standard deviations in the least significant figure(s) are given in parentheses in this and all subsequent tables. The form of the anisotropic thermal ellipsoid is $\exp[-2\pi^2(U_{11}h^2a^{*2} + U_{22}k^2b^{*2} + U_{33}l^2c^{*2} + 2U_{12}hka^*b^* + 2U_{13}hla^*c^* + 2U_{23}klb^*c^*)]$. The quantities given in the table are the thermal coefficients $\times 10^2$.

from the five nearest atoms bonded to the iridium atoms. Other peaks are featureless.

The correctness of the centrosymmetric $P\bar{1}$ space group used in our calculations is supported by quite normal vibrational ellipsoids (Table II) although those of the fluorine of CF_3 groups are rather large. The fact that the H atoms could be located on a difference Fourier map is perhaps the strongest evidence that the correct space group was used. There is no reason indeed to believe that one would expect to find H atoms of the CH_3 groups if the correct space group was $P1$.

The final positional and thermal parameters (B's or U_{ij}) of all nonhydrogen atoms appear in Table II. The idealized positions of H atoms are shown in Table III. The observed and calculated structure amplitudes for the data used are available as supplementary material.

Table III. Idealized Positions of the Hydrogen Atoms

atoms	x	y	z	B, Å^2
HA(12)	−0.173	0.344	0.081	6.6
HB(12)	−0.047	0.285	0.060	6.6
HC(12)	−0.063	0.421	0.066	6.6
HA(13)	−0.246	0.189	−0.106	5.9
HB(13)	−0.177	0.165	−0.236	5.9
HC(13)	−0.120	0.130	−0.119	5.9
HA(14)	−0.255	0.416	−0.080	6.7
HB(14)	−0.141	0.469	−0.126	6.7
HC(14)	−0.212	0.366	−0.223	6.7
HA(16)	0.344	0.430	−0.588	6.1
HB(16)	0.394	0.343	−0.513	6.1
HC(16)	0.266	0.324	−0.572	6.1
HA(17)	0.408	0.584	−0.380	5.8
HB(17)	0.337	0.587	−0.256	5.8
HC(17)	0.428	0.483	−0.312	5.8
HA(18)	0.210	0.571	−0.507	6.6
HB(18)	0.114	0.499	−0.456	6.6
HC(18)	0.177	0.610	−0.361	6.6

Results and Discussion

A perspective view of the $Ir_3(\mu\text{-}S\text{-}t\text{-}Bu)_3(\mu\text{-}C_4F_6)(CO)_6$ molecule, including the labeling scheme, is shown in Figure 1. The molecular skeleton can be described as a six-membered ring of alternate Ir and S atoms in a chair conformation with a bridge built from atoms Ir(1)–C(20)–C(22) and Ir(2). Atoms Ir(1), S(2), S(3), and Ir(2) are coplanar; Ir(3) and S(1) are respectively above and below this mean plane (Table IV). Moreover, the molecular skeleton roughly accepts a mirror plane passing through S(1) and Ir(3) atoms and perpendicular to the Ir(1)–Ir(2) direction.

Geometry around Ir(3) is of usual square-planar type for iridium(I). Geometry around Ir(1) and Ir(2) is of rectangular

Table IV. Least-Squares[a] Planes and Dihedral Angles in $Ir_3(\mu\text{-S-}t\text{-Bu})_3(\mu\text{-}C_4F_6)(CO)_6$

Least-Squares Planes

atom	dist from plane, Å	atom	dist from plane, Å
Plane 1:	$0.4443X + 0.2917Y + 0.8471Z + 0.1049 = 0$		
Ir(1)	−0.002 (2)	S(3)	−0.001 (2)
Ir(2)	0.005 (2)	Ir(3)	−1.799
S(2)	0.005 (2)	S(1)	1.903
Plane 2:	$0.4125X - 0.8989Y - 0.1480Z + 3.5595 = 0$		
S(2)	0.014 (2)	C(6)	−0.016 (2)
S(3)	−0.013 (2)	Ir(3)	0.029
C(5)	0.016 (2)		
Plane 3:	$0.4680X + 0.2215Y + 0.8555Z + 0.2665 = 0$		
Ir(1)	0.018 (2)	C(20)	−0.020 (2)
Ir(2)	−0.022 (2)	C(22)	0.019 (2)
Plane 4:	$0.5903X - 0.7886Y + 0.1725Z + 1.1663 = 0$ Calculated from Ir(1), Ir(2), and S(1) atom positions		

Dihedral Angles

plane	plane	dihedral angle, deg
1	2	101.8
1	3	4.3
1	4	100.3

[a] Least-squares planes are defined by atoms for which a standard deviation is given in parentheses. X, Y, Z are orthogonal coordinates (in Å) related to fractional coordinates x, y, z by $X = ax \sin\gamma$, $Y = by$, $Z = cz \sin\alpha$.

Table V. Signed Conformational (Torsion) Angles (deg) in $Ir_3(\mu\text{-S-}t\text{-Bu})_3(\mu\text{-}C_4F_6)(CO)_6$

S(1)-Ir(1)-S(2)-C(11)	−134.5 (4)
S(1)-Ir(2)-S(3)-C(15)	133.1 (4)
S(2)-Ir(1)-S(1)-C(7)	145.5 (4)
S(3)-Ir(2)-S(1)-C(7)	−147.6 (5)
S(2)-C(11)-C(12)-HA(12)	177 (1)
S(2)-C(11)-C(12)-HB(12)	−64 (1)
S(2)-C(11)-C(12)-HC(12)	57 (1)
S(2)-C(11)-C(13)-HA(13)	180 (1)
S(2)-C(11)-C(13)-HB(13)	−60 (1)
S(2)-C(11)-C(13)-HC(13)	61 (1)
S(2)-C(11)-C(14)-HA(14)	−160 (1)
S(2)-C(11)-C(14)-HB(14)	−41 (1)
S(2)-C(11)-C(14)-HC(14)	80 (1)
S(3)-C(15)-C(16)-HA(16)	170 (1)
S(3)-C(15)-C(16)-HB(16)	−71 (1)
S(3)-C(15)-C(16)-HC(16)	50 (1)
S(3)-C(15)-C(17)-HA(17)	−177 (1)
S(3)-C(15)-C(17)-HB(17)	−57 (1)
S(3)-C(15)-C(17)-HC(17)	62 (1)
S(3)-C(15)-C(18)-HA(18)	−165 (1)
S(3)-C(15)-C(18)-HB(18)	−45 (1)
S(3)-C(15)-C(18)-HC(18)	75 (1)

pyramidal type if one considers the five nearest atoms around each iridium.

Despite the presence of the C_4F_6 bridge, the *t*-Bu group on S(1) is in equatorial position. To avoid repulsion, the bulky *t*-Bu groups on S(2) and S(3) are also in equatorial positions; both of them adopt two conformations in which three C–H bonds are parallel to the S–C direction (see Table V).

Atoms Ir(1), C(20), C(22), and Ir(2) are coplanar and their mean plane forms a dihedral angle of only 4.3° with the Ir(1)Ir(2)S(2)S(3) plane.

Distances and angles of interest are listed in Table VI. In this trinuclear complex, two iridium atoms are close to each other (Ir(1)–Ir(2) = 2.692 (1) Å) in contrast with the two others, Ir(1)–Ir(3) and Ir(2)–Ir(3) (3.571 (1) and 3.619 (1) Å, respectively). By comparison with the other two sulfur linkages, it is obvious that the S(1)-*t*-Bu link is not responsible for the short Ir(1)–Ir(2) observed distance. One might guess

Table VI. Selected distances (Å) and Angles (deg)

Ir(1)-Ir(2)	2.692 (1)	C(4)-O(4)	1.11 (1)
Ir(1)-Ir(3)	3.571 (1)	C(5)-O(5)	1.12 (2)
Ir(1)-S(1)	2.361 (3)	C(6)-O(6)	1.13 (1)
Ir(1)-S(2)	2.466 (2)	C(7)-C(8)	1.52 (3)
Ir(1)-O(1)	3.03 (1)	C(7)-C′(8)	1.47 (3)
Ir(1)-O(2)	3.016 (8)	C(7)-C(9)	1.57 (3)
Ir(1)-C(1)	1.90 (1)	C(7)-C′(9)	1.53 (3)
Ir(1)-C(2)	1.88 (1)	C(7)-C(10)	1.51 (4)
Ir(1)-C(20)	2.08 (1)	C(7)-C′(10)	1.63 (4)
Ir(2)-Ir(3)	3.619 (1)	C(11)-C(12)	1.53 (2)
Ir(2)-S(1)	2.349 (3)	C(11)-C(13)	1.53 (2)
Ir(2)-S(3)	2.464 (3)	C(11)-C(14)	1.51 (2)
Ir(2)-O(3)	3.052 (9)	C(15)-C(16)	1.53 (2)
Ir(2)-O(4)	3.016 (8)	C(15)-C(17)	1.54 (2)
Ir(2)-C(3)	1.91 (1)	C(15)-C(18)	1.51 (2)
Ir(2)-C(4)	1.90 (1)	C(19)-C(20)	1.50 (2)
Ir(2)-C(22)	2.08 (1)	C(19)-F(1)	1.27 (2)
Ir(3)-S(2)	2.379 (3)	C(19)-F(2)	1.30 (2)
Ir(3)-S(3)	2.381 (2)	C(19)-F(3)	1.28 (2)
Ir(3)-O(5)	2.97 (1)	C(20)-C(22)	1.29 (1)
Ir(3)-O(6)	2.979 (9)	C(21)-C(22)	1.52 (1)
Ir(3)-C(5)	1.85 (1)	C(21)-F(4)	1.27 (2)
Ir(3)-C(6)	1.85 (1)	C(21)-F(5)	1.29 (1)
S(1)-C(7)	1.86 (1)	C(21)-F(6)	1.33 (2)
S(2)-C(11)	1.87 (1)		
S(3)-C(15)	1.86 (1)		
C(1)-O(1)	1.13 (1)		
C(2)-O(2)	1.13 (1)		
C(3)-O(3)	1.14 (1)		
S(1)-Ir(1)-S(2)	84.51 (8)	S(2)-Ir(3)-S(3)	79.16 (8)
S(2)-Ir(1)-C(2)	91.8 (3)	S(3)-Ir(3)-C(5)	96.8 (4)
C(2)-Ir(1)-C(20)	87.7 (4)	C(5)-Ir(3)-C(6)	86.7 (6)
C(20)-Ir(1)-S(1)	90.4 (3)	C(6)-Ir(3)-S(2)	97.4 (4)
S(1)-Ir(1)-C(2)	158.8 (4)	Ir(1)-S(1)-Ir(2)	69.70 (7)
S(2)-Ir(1)-C(20)	164.7 (3)	Ir(2)-S(1)-C(7)	120.6 (4)
C(1)-Ir(1)-S(1)	101.1 (4)	C(7)-S(1)-Ir(1)	120.6 (4)
C(1)-Ir(1)-S(2)	99.2 (4)	Ir(1)-S(2)-Ir(3)	94.94 (9)
C(1)-Ir(1)-C(2)	100.2 (5)	Ir(3)-S(2)-C(11)	116.5 (4)
C(1)-Ir(1)-C(20)	95.9 (5)	C(11)-S(2)-Ir(1)	113.6 (4)
S(1)-Ir(2)-S(3)	85.26 (9)	Ir(2)-S(3)-Ir(3)	96.7 (1)
S(3)-Ir(2)-C(4)	92.6 (3)	Ir(3)-S(3)-C(15)	115.9 (4)
C(4)-Ir(2)-C(22)	88.2 (5)	C(15)-S(3)-Ir(2)	115.6 (4)
C(22)-Ir(2)-S(1)	89.4 (3)	Ir(1)-C(20)-C(19)	120.7 (8)
S(1)-Ir(2)-C(4)	157.6 (3)	C(19)-C(20)-C(22)	129 (1)
S(3)-Ir(2)-C(22)	162.7 (3)	C(22)-C(20)-Ir(1)	109.7 (8)
C(3)-Ir(2)-S(1)	103.1 (4)	Ir(2)-C(22)-C(20)	109.6 (7)
C(3)-Ir(2)-S(3)	97.5 (3)	C(20)-C(22)-C(21)	126 (1)
C(3)-Ir(2)-C(4)	99.3 (5)	C(21)-C(22)-Ir(2)	123.8 (9)
C(3)-Ir(2)-C(22)	99.4 (4)		

that the phenomenon is due to the C_4F_6 bridge for purely steric reasons, but a straight-forward calculation based on a C(20)–C(22) bond length of 1.30 Å, Ir–C bond length of 2.10 Å, and angles of 120° around the two carbon atoms of the C=C bond leads to an Ir(1)–Ir(2) distance of 3.40 Å. Furthermore, such a calculated geometry would permit a larger value for the Ir(1)–S(1)–Ir(2) angle, i.e., less constraint for the S(1) atom. It would lead also to smaller values for the trans-basal angles in each rectangular pyramid around the two concerned Ir atoms which would be then closer to the ideal model. It thus appears that the short Ir(1)–Ir(2) distance is due to an important metal–metal interaction. Such a proposal is comforted by the comparison of the observed distances in dinuclear complexes of Ir and Rh[9] in which metal–metal bonds have been assumed.

Due to the Ir–Ir bond, the geometry around the Ir atom should be between a rectangular pyramid (pentacoordination) and the octahedron (hexacoordination). Taking into account the complexity of the structure, we felt it would have been inadequate to undertake an accurate calculation based upon

(9) R. S. Dickson, H. P. Kirsch, and D. J. Lloyd, *J. Organomet. Chem.*, **101**, C48 (1975).

Table VII. Comparison of Some Bond Angles around Ir(1) and Ir(2) in Compound III with Those Assumed for SP and HO Geometries

	square pyramid (ideal geometry)	obsd angles around Ir(1), deg	obsd angles around Ir(2), deg	half-octahedron (ideal geometry)
trans basal	156	158.8 (4)	157.6 (3)	180
	156	164.7 (3)	162.7 (3)	180
apical basal	102	101.1 (4)	103.1 (4)	90
	102	99.2 (4)	97.5 (3)	90
	102	100.2 (5)	99.3 (5)	90
	102	95.9 (5)	99.4 (4)	90

dihedral angles of the polyhedra around Ir(1) and Ir(2).[10] Nevertheless, the trans-basal and apical-basal angles are between an ideal rectangular pyramid and octahedron (Table VII).

Finally, structural results give strong evidence of a metal–metal bond between Ir(1) and Ir(2). This is quite consistent with an oxidative addition of the alkyne ligand to two iridium(I) atoms: indeed, the C(20)–C(22) bond distance is significantly longer than in free alkyne. The oxidative process simultaneously occurring on two metal atoms formally leads to an increase of only one unit of the oxidation number of each Ir atom which could be considered in the formal oxidation state II.

Therefore, the formation of a metal–metal bond reintroduces the spin pairing of electrons after fixation of C_4F_6, which is consistent with the observed diamagnetism.

Syntheses and Structures in Solution. The formation of complexes III and IV from I when a pentane solution of alkyne is added was followed by infrared spectroscopy. In each case, during the reaction, six new CO bands appear. If the initial ratio of I:alkyne was fixed close to 3:2, these bands remained alone in the infrared spectra at the end of the reaction. The ^1H NMR spectrum of the isolated product presents two signals in 1:2 ratio for the *tert*-butyl proton, whereas the ^{19}F NMR spectrum gives a single signal (Table VIII). Therefore, these observations coupled with molecular weight are consistent with the formation of a complex formulated as $Ir_3(\mu\text{-S-}t\text{-Bu})_3(\mu\text{-}C_4F_6)(CO)_6$. This complex is very soluble in all organic solvents (pentane, C_6H_6, CH_2Cl_2, ...) but alcohols.

The structure observed in the crystal allows one to rationalize the preceding data in solution, in terms of a C_s local symmetry for the six CO groups. Moreover, as Ir(1) and Ir(2) atoms were considered as being in the II oxidation state and Ir(3) remaining in the I state, a shift can be expected between the mean frequency of the two CO modes attributed to the group $Ir(3)(CO)_2$ and the mean frequency of the four CO modes attributed to the dinuclear group $Ir(1)Ir(2)(CO)_4$ in the molecule. Such an expectation obviously neglects the possible couplings between the two kinds of modes but seems quite reasonable. Therefore we can assign to the symmetric and antisymmetric CO modes of the group $Ir(3)^I(CO)_2$ a couple of bands in the lower frequency part of the CO stretching spectrum, the frequency separation of which is around the 60 cm^{-1} generally observed for geminal CO groups in square-planar iridium complexes[11] (namely, in the cases of compound III, 1983 and 2040 cm^{-1} or 1983 and 2048 cm^{-1}, and compound IV, 1977 and 2033 cm^{-1} or 1977 and 2042 cm^{-1}). The two inequivalent *tert*-butyl proton signals observed by NMR are also compatible with a structure in solution identical with the one determined in the crystal.

(10) E. L. Muetterties and J. L. Guggenberger, *J. Am. Chem. Soc.*, **96**, 1748 (1974).
(11) M. I. Bruce, B. L. Goodall, M. Z. Iqbal, and F. G. A. Stone, *Chem. Commun.*, 661 (1971); A. Maisonnat, P. Kalck, and R. Poilblanc, *Inorg. Chem.*, **13**, 661 (1974).

Table VIII. Infrared and ^1H and ^{19}F NMR Data for the Complexes I–VI

complex	ν_{CO},[a] cm^{-1}	$\nu_{C=C}$,[b] cm^{-1}	^1H[c] δ_{SR}	^1H[c] δ_{OCH_3}	^1H[c] $\delta_{P(OCH_3)_3}$	$J_{P(OCH_3)_3}$[d]	^{19}F[e]
$[IrSC(CH_3)_3(CO)_2]_2$ (I)	2061 s, 2040 vs, 1986 vs		−1.67				
$[IrSC(CH_3)_3(CO)P(OCH_3)_3]_2$ (II)	1985 vs, 1975 vs, 1965 vs		−1.63 (1)		−4.80	12.0	
$Ir_3(SC(CH_3)_3)_3(CO)_6(C_4F_6)$ (III)	2089 s, 2072 vs, 2048 vs, 2038 s, 2029 m, 1983 vs	1620	−1.27 (2)				−25.2
			−1.29 (1)				
$Ir_3(SC(CH_3)_3)_3(CO)_6(C_2(CO_2CH_3)_2)$ (IV)	2084 s, 2066 vs, 2042 vs, 2033 s, 2021 m, 1977 vs	1601	−1.33 (2)	−3.49			
			−1.47 (1)				
$[IrSC(CH_3)_3(CO)P(OCH_3)_3]_2(C_4F_6)$ (V)	2030 vs, 2010 m	1595	−1.32 (1)		−3.52	12.6	−25.2
			−1.38 (1)				
$[IrSC(CH_3)_3(CO)P(OCH_3)_3]_2(C_2(CO_2CH_3)_2)$ (VI)	2012 vs, 1988 s	1567	−1.40 (1)	−3.61	−3.64	12.5	
			−1.43 (1)				

[a] In hexadecane solutions. [b] In CsBr pellet. [c] In ppm from Me_4Si as internal standard in C_6H_6 solution. [d] In Hz. [e] In ppm from CF_3COOH as internal standard in C_6H_6 solution.

In order to protonate the metal–metal bond,[12] we added concentrated $HClO_4$ to a solution of complexes III and IV, but the starting material remained unchanged. This is attributed to a low basicity of these complexes.

Addition of Alkynes to Substituted Dinuclear Iridium Complexes. In contrast with the case of complex I, addition of 1 equiv of C_4F_6 or $C_2(CO_2CH_3)_2$ to complex II causes immediate formation of complexes V and VI, respectively. Infrared data, ^1H NMR spectra (Table VIII), molecular weights, and elemental analysis are consistent with the formation of dimetallic complexes formulated: $[Ir_2(\mu\text{-S-}t\text{-Bu})_2(\mu\text{-}C_4F_6)(CO)_2(P(OCH_3)_3)_2]$ (V) and $[Ir_2(\mu\text{-S-}t\text{-Bu})_2(\mu\text{-}C_2(CO_2CH_3)_2(CO)_2(P(OCH_3)_3)_2]$ (VI).

According to ^1H and ^{19}F NMR data, the $-CF_3$ and $-OCH_3$ groups are equivalent and play in these compounds (V and VI) a symmetric role with respect to the pair of iridium atoms. The C–C bond especially is either perpendicular[2] or parallel[3] to the metal–metal axis. By comparison with the trinuclear complexes (III and IV) in which the second proposal is demonstrated, it is admitted here that the alkyne ligand is also σ bonded to both iridium atoms, in the formal II oxidation state, the diamagnetism implying the existence of a metal–metal bond. In fact, the ν_{CO} stretching frequency values are quite consistent with an oxidative addition on a couple of iridium(I) atoms. Furthermore, the low $\nu_{C=C}$ frequency ($\sim$1600 cm^{-1}) in these compounds has never been observed for the C=C bond when perpendicular, and we must admit that it is characteristic of a C=C bond parallel to the metal–metal axis.[3] Although no crystallographic study is yet available, a structure can be tentatively proposed.

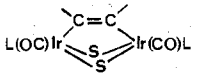

Acknowledgment. We wish to thank Mr. A. Mari for magnetic measurements and the CNRS, DES, and DGRST for their financial support.

Registry No. I, 63312-27-6; II, 63292-76-2; III, 71661-72-8; IV, 71661-71-7; V, 69206-36-6; VI, 71661-70-6.

Supplementary Material Available: A listing of structure factor amplitudes (17 pages). Ordering information is given on any current masthead page.

(12) A. Thorez, A. Maisonnat, and R. Poilblanc, *J. Chem. Soc., Chem. Commun.*, 518 (1977).

Contribution from the Department of Chemistry, The University of Texas at Austin, Austin, Texas 78712

Crystal Structures at −35 °C of Tetraphenylphosphonium (Triphenylphosphino)tetracarbonylmanganate and (Triphenylphosphino)tetracarbonyliron

PAUL E. RILEY and RAYMOND E. DAVIS*

Received March 29, 1979

The structures of $[Ph_4P][Mn(CO)_4PPh_3]$ and $Fe(CO)_4PPh_3$ (Ph = C_6H_5) have been determined by single-crystal X-ray diffraction techniques with three-dimensional data gathered at −35 °C by counter methods. Deep red, block-like single crystals of $[Ph_4P][Mn(CO)_4PPh_3]$ form in monoclinic space group $P2_1/c$ with unit cell constants (at −35 °C) a = 10.735 (3) Å, b = 17.412 (4) Å, c = 20.847 (8) Å, and β = 99.16 (2)°. The calculated density of 1.332 g cm^{-3} is reasonable for four formula weights of $[Ph_4P][Mn(CO)_4PPh_3]$ per unit cell. $Fe(CO)_4PPh_3$ crystallizes as yellow plates in triclinic space group $P\bar{1}$ with unit cell constants (at −35 °C) a = 10.348 (2) Å, b = 10.709 (7) Å, c = 9.809 (6) Å, α = 112.73 (5)°, β = 94.39 (2)°, and γ = 90.12 (2)°. The calculated density of 1.436 g cm^{-3}, assuming two molecules of $Fe(CO)_4PPh_3$ per unit cell, agrees satisfactorily with the measured value of 1.41 g cm^{-3}. Full-matrix least-squares refinements of the structures have converged with conventional R indices (on $|F|$) of 0.077 and 0.061 for $[Ph_4P][Mn(CO)_4PPh_3]$ and $Fe(CO)_4PPh_3$, respectively, using (in the same order) the 4189 and 3961 symmetry-independent reflections with $I_o > 2.0\sigma(I_o)$. In each metal complex the PPh_3 ligand occupies an axial position of a distorted trigonal bipyramid, such that the resulting ML_4L' complexes exhibit approximate C_{3v} symmetry. The average lengths of the M–C bonds in these ML_4L' structures are substantially shorter than those of the parent ML_5 complexes and are equal despite differences in charge and metal atom size. In the Mn structure the axial Mn–C bond shows the larger contraction from the value determined for the unsubstituted complex, suggesting that the PPh_3 substituent exerts a trans stabilizing influence upon the axial CO ligand. In $[Mn(CO)_4PPh_3]^-$, the equatorial Mn–C distances are equal to the corresponding distances in $[Mn(CO)_5]^-$, implying that the π-acceptor orbitals of the equatorial CO ligands are already nearly saturated from the negative charge of the complex. The changes in bond lengths upon phosphine substitution are consistent with the changes in carbonyl stretching force constants and with the reluctance of $[Mn(CO)_4PPh_3]^-$ to undergo additional phosphine substitution. In the two Fe complexes, the equatorial Fe–C bonds show the larger contraction upon phosphine substitution, suggesting that in $Fe(CO)_5$ the π-acceptor orbitals of these CO ligands are not saturated.

Introduction

It has long been established that for trigonal-bipyramidal molecules which possess five equivalent ligands a difference between axial and equatorial bond lengths is generally observed. The explanations offered for this, (1) repulsions between valence shell electron pairs and/or (2) repulsions between valence shell electrons and electrons of partially filled d shells of transition metal atoms (i.e., nonspherical d-electron clouds), have been discussed at length elsewhere.[1,2] Low-spin d^7, d^8, and d^9 metal complexes are of particular interest, because for trigonal-bipyramidal geometry the metal d_{z^2} orbital is either empty or half-filled. Hence, such electron clouds are oblate ellipsoidal, favoring axial bonds which are shorter than equatorial bonds. Furthermore, within an isoelectronic series of trigonal-bipyramidal transition metal complexes of the form ML_5, it has been noted that the difference between axial and equatorial bond lengths decreases with decreasing charge on the metal,[3,4] presumably a result of increased d-electron–valence shell electron repulsion.

(1) R. J. Gillespie, *J. Chem. Soc.*, 4672, 4679 (1963).
(2) A. R. Rossi and R. Hoffmann, *Inorg. Chem.*, **14**, 365 (1975).
(3) B. A. Frenz and J. A. Ibers in "The Biennial Review of Chemistry, Chemical Crystallography", J. M. Robertson, Ed., Medical and Technical Publishing Co., Aylesburg, England, 1972, Chapter 2, and references therein.
(4) B. A. Frenz and J. A. Ibers, *Inorg. Chem.*, **11**, 1109 (1972).

0020-1669/80/1319-0159$01.00/0